Vibrational relaxation of CH_2I_2 in solution: Excitation level dependence

Christopher G. Elles, Dieter Bingemann, Max M. Heckscher, and F. Fleming Crim[a)]
Department of Chemistry, University of Wisconsin-Madison, Madison, Wisconsin 53706

(Received 15 November 2002; accepted 31 December 2002)

Transient electronic absorption monitors the flow of vibrational energy in methylene iodide (CH_2I_2) following excitation of five C–H stretch and stretch–bend modes ranging in energy from 3000 to 9000 cm^{-1}. Intramolecular vibrational relaxation (IVR) occurs through a mechanism that is predominantly state-specific at the C–H stretch fundamental but closer to the statistical limit at higher excitation levels. The IVR times change with the excitation energy between the fundamental and first C–H stretch overtone but are constant above the overtone. The intermolecular energy transfer (IET) times depend only weakly on the initial excitation level. Both the IVR and the IET times depend on the solvent [CCl_4, $CDCl_3$, C_6D_6, C_6H_6, or $(CD_3)_2CO$] and its interaction strength, yet there is no energy level dependence of the solvent influence. © *2003 American Institute of Physics.* [DOI: 10.1063/1.1554396]

I. INTRODUCTION

Vibrational energy plays a major role in every chemical reaction. Since nuclear motion transforms reactants into products, the rate, and even the outcome, of a reaction depends on the amount and distribution of vibrational energy.[1,2] The vibrational dynamics are therefore ultimately responsible for the evolution of a reactive system, and the processes that move energy within and out of a molecule play an essential role. Short-pulse lasers can directly follow this flow of energy by exciting a specific vibrational motion and monitoring the transient response of the molecule,[3–5] providing a test for theoretical treatments of vibrational energy transfer.[6–8] In the work described here we examine the influence of the excitation level on vibrational relaxation for a wide range of initial vibrational energies.

Intramolecular vibrational relaxation (IVR) is the process by which energy flows within a molecule.[9–11] Anharmonic coupling between the initially excited state and each of the energetically available states governs the redistribution of energy since the energy transfer rate increases with coupling strength. Only one or a few states dominate the initial relaxation in the state-specific limit, while in the statistical limit the relaxation involves a very large number of accepting states. During state-specific IVR, energy initially flows into only the most strongly coupled states, while relaxation into other energetically accessible states occurs more slowly. This situation can result in oscillating populations if energy returns to the initially excited state before it flows into a large number of the weakly coupled modes or the surroundings.[9] In contrast, statistical IVR *directly* populates every accessible state, resulting in a monotonic population decay of the initially excited state and a uniform distribution of energy within the molecule.[12] The number of vibrational states in a molecule increases rapidly with the energy level, providing a means of studying the relationship between the density of states, ρ, and the IVR mechanism. For example, experiments that prepare gas phase molecules with varying amounts of vibrational energy above the S_1 electronic origin show a transition from state-specific IVR at low levels of vibrational excitation to a statistical relaxation mechanism at high excitation energies, where the density of states is much larger.[13–18]

The rate of intramolecular relaxation, τ_{IVR}^{-1}, depends on the density of states because it limits the number of available energy transfer pathways. For a statistical relaxation mechanism, Fermi's Golden Rule[19] gives the IVR rate in terms of ρ,

$$\tau_{IVR}^{-1} = 4\pi^2 c \rho |V|^2, \tag{1}$$

where the coupling strength, V, to the initially excited state is the same for all of the states that accept energy. Experiments often show, however, that the IVR rate does not scale with the total density of states.[20–25] Such a deviation from Fermi's Golden Rule occurs when only a fraction of the available states participate in the initial energy transfer. Separating the accepting states into tiers according to their coupling strength accounts for the larger role that some states play in the relaxation compared to others.[10,11,26] The excited state initially transfers energy to only those states in the first tier, which contains the most strongly coupled states, and then on a slower time scale the energy relaxes into the remaining, more weakly coupled states. This picture recovers the limiting mechanisms of state-specific IVR, where only a few states are in the first tier, and of statistical IVR, where a large number of states compose the first tier.

The vibrational relaxation process is even more complicated in solution,[27–40] where *inter*molecular energy transfer (IET) to the solvent is important. IET depends on the internal vibrational modes of the solute, as well as the surrounding environment, since some modes transfer energy to the solvent more effectively than others. Vibrational energy generally flows *within* the molecule until it reaches these ''gateway'' modes, which then efficiently transfer the energy to solution. It is also possible that the intra- and intermolecular energy relaxation occurs simultaneously. The low frequency

a)Electronic mail: fcrim@chem.wisc.edu

collective modes of the solvent can accelerate the intramolecular relaxation by making up small energy differences between an initially excited state and the accepting states.[7,41,42] This solvent-assisted IVR depends strongly on the solvent environment.

In the present work we examine IVR and IET in methylene iodide (CH_2I_2) following excitation of five different C–H stretch and stretch–bend states ranging in energy from 3000 to 9000 cm^{-1}. Graener and Laubereau[30] and Bakker *et al.*[34] were the first to study vibrational relaxation of CH_2I_2 following picosecond excitation of the C–H stretch fundamental vibrations, and their results indicate a state-specific IVR mechanism. Our recent work[43–45] suggests that the IVR mechanism changes between the C–H stretch fundamental and the first overtone, and Abel and co-workers[46,47] show that the IVR rate does not scale with the total density of states between the stretch–bend combination region and the stretch overtone. The past studies also show that the IET rate depends on the initial excitation level and that the solvent influences the rates of both IVR and IET. Here we investigate a wider range of excitation levels and explore systematically the influence of the excitation level on the IVR mechanism, the IVR and IET times, and the solvent dependence of the relaxation.

II. EXPERIMENT

We monitor the vibrational relaxation of CH_2I_2 in solution by observing the time-dependent change in electronic absorption following vibrational excitation. This detection technique is only sensitive to motion along the Franck–Condon active (primarily C–I stretch) vibrational modes, whose excitation increases the electronic absorption at long wavelengths. Figure 1 shows a schematic diagram of the experimental approach and a typical transient absorption trace. A short laser pulse excites a C–H vibration, which does not enhance the absorption in the long-wavelength portion of the electronic absorption spectrum since it is Franck–Condon inactive. During intramolecular vibrational relaxation, energy flows into states with some excitation in the C–I stretching coordinate, and the electronic absorption in the long-wavelength part of the spectrum increases, as shown in the experimental transient in Fig. 1. The subsequent intermolecular equilibration with the solvent lowers the total energy of the solute, depopulating the excited Franck–Condon active modes and decreasing the transient absorption.

We vibrationally excite CH_2I_2 with 100-fs mid-infrared or near-infrared pump pulses tuned to one of the C–H stretch or stretch–bend bands shown in the spectrum of Fig. 2, where ν_s and ν_b denote the C–H stretch and H–C–H bend, respectively. (This notation ignores the relative contribution of specific normal modes to each bright state since the laser excites all transitions that lie within the pulse bandwidth.) The pump pulses come from nonlinear frequency conversion of 800 nm pulses from a regeneratively amplified Ti:sapphire laser (Clark MXR CPA-1000) that delivers a 1 kHz train of 100 fs pulses at an energy of 1 mJ. Approximately 50% of the light from the Ti:sapphire laser pumps a continuum seeded optical parametric amplifier (OPA) based on a 5 mm, type-II β-barium borate (BBO) crystal cut at $\theta = 27°$. We separate the signal and idler beams of the OPA with a polarizer and use them directly for the near-infrared pump pulses in the wavelength range from 1.1 to 2.5 μm (9000 to 4000 cm^{-1}). Difference frequency mixing of the signal and idler pulses from the OPA in a 1 mm, type-II silver gallium sulfide ($AgGaS_2$) crystal cut at $\theta = 50°$ generates midinfrared pump pulses at 3.3 μm (3000 cm^{-1}).[44] The pump pulse energy varies from approximately 2 to 40 μJ depending on the wavelength. Two successive type-I BBO crystals (1 mm, θ

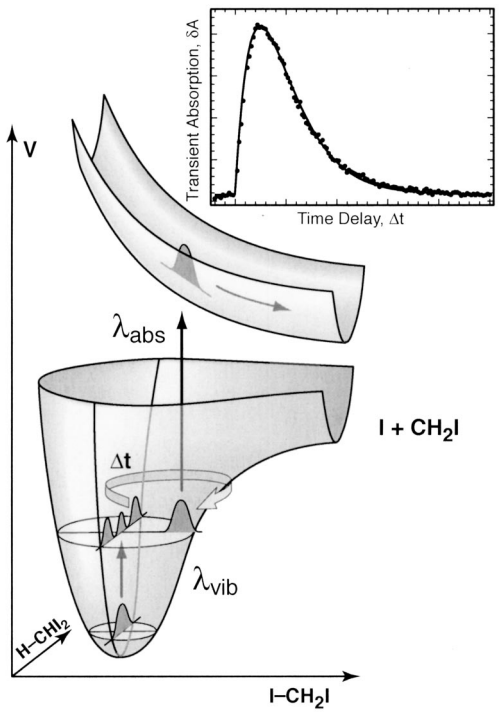

FIG. 1. Schematic diagram of the transient electronic absorption technique for CH_2I_2. Absorption of an infrared photon with wavelength λ_{vib} (3.3–1.1 μm) excites a nonstationary C–H stretch or stretch–bend state. Following time delay Δt, absorption at the probe wavelength λ_{abs} (360–400 nm) measures excitation in the Franck–Condon active (primarily C–I stretch) modes. The inset is a sample experimental trace showing the rise and decay of the absorption at λ_{abs}.

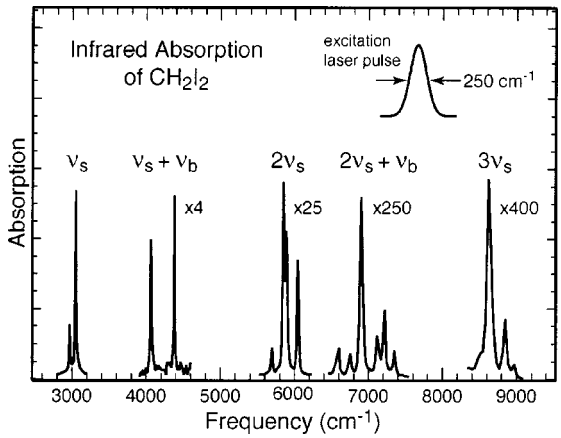

FIG. 2. Infrared absorption spectrum of the C–H stretch (ν_s) and bend (ν_b) modes for CH_2I_2 in the region 3000 to 9000 cm^{-1}. The excitation laser pulses, also represented in the figure, have a bandwidth of approximately 250 cm^{-1}.

$=22°$, and 0.3 mm, $\theta=29°$) frequency quadruple the signal pulse from a second BBO OPA, pumped with approximately 30% of the light from the Ti:sapphire laser, to generate ultraviolet probe pulses at 390 nm and below. We frequency double a portion of the remaining Ti:sapphire light directly to produce 400 nm probe pulses.

A computer controlled translation stage adjusts the delay between the pump and probe pulses, and a metal-coated parabolic mirror with 100 mm focal length focuses the pump beam to a 100 μm diameter in the sample. The probe beam, which a 120 mm lens focuses to a similar size, intersects the pump beam at a small angle in the sample. Two silicon photodiodes measure the probe pulse energy before and after the sample to account for fluctuations in the laser intensity, and a synchronized chopper blocks every other pump pulse for active background subtraction. Averaging between 1000 and 10 000 laser shots per delay step produces a detection limit of about 0.01 mOD. We make 1 M solutions of CH_2I_2 in CCl_4, $CDCl_3$, C_6D_6, C_6H_6, and $(CD_3)_2CO$ using the reagents as received, without further purification. The solution circulates through a 6 mm$\times$300 μm nozzle to form a 250 μm thick liquid jet with the flow rate set to minimize fluctuations in the recorded probe beam intensity.

III. RESULTS AND DISCUSSION

A. Intramolecular vibrational relaxation mechanism

The two limiting cases of intramolecular vibrational relaxation are the state-specific and the statistical mechanisms, an important distinction since the mechanism governs the redistribution of energy throughout the molecule. Traditional methods for determining the IVR mechanism, such as high resolution spectroscopy,[10] are impractical in solution because of interactions with and energy transfer to the solvent. Our infrared pump and ultraviolet probe technique, however, distinguishes between the two limiting IVR mechanisms through the wavelength dependence of the decay times of the transient electronic absorption.

State-specific intramolecular vibrational relaxation from the initially excited state populates only one or a few accepting states. These states contain only low levels of excitation in the Franck–Condon active coordinates since transitions with a small change in quantum number should dominate the initial energy transfer. In the limit that subsequent relaxation steps do not further excite the Franck–Condon active modes, the low-lying states dominate the transient electronic absorption at all wavelengths, as shown schematically in the top portion of Fig. 3. The transient absorption directly monitors the population evolution of the newly populated states independent of the wavelength, and the decay time is the same for all probe wavelengths.[44,45]

The limit of statistical intramolecular vibrational relaxation produces a very different picture, as outlined in the bottom part of Fig. 3. This mechanism populates not a single accepting state, but a statistical ensemble of all modes in the molecule. The population distribution in the Franck–Condon active modes shifts to higher levels of excitation as the initially excited state relaxes and returns to lower levels during energy transfer to the solvent. During the cooling process,

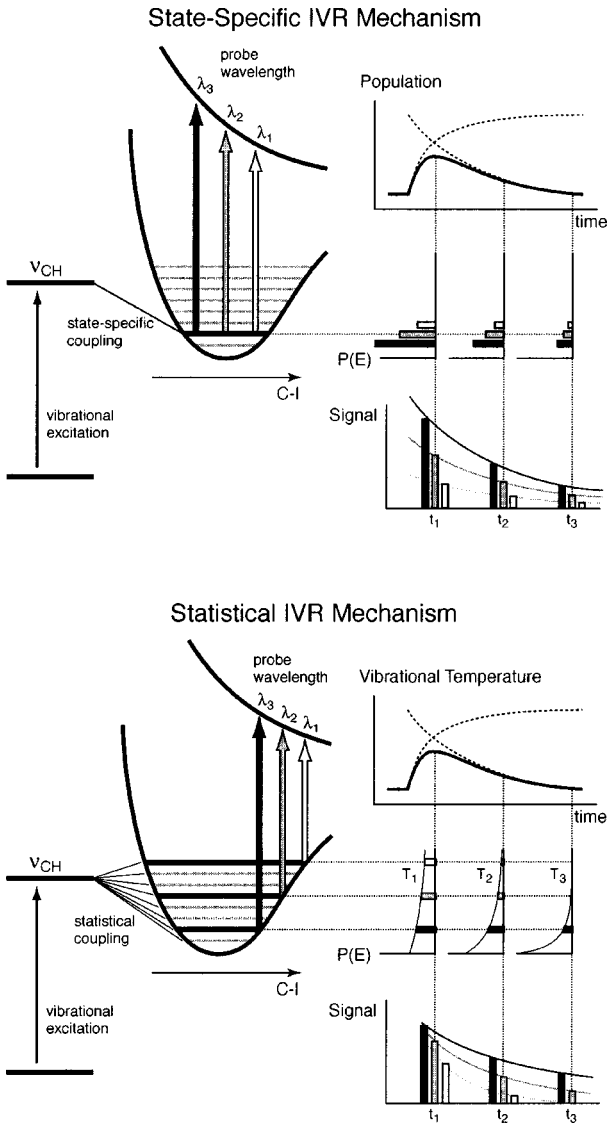

FIG. 3. Top: diagram of the population evolution for a single Franck–Condon active state populated through state-specific IVR from the initially excited C–H mode. Bottom: diagram of the vibrational temperature evolution following statistical IVR. Note that the signal decay depends on the probe wavelength in the bottom panel but not the top.

the vibrational population decays more rapidly for highly excited states relative to those with fewer quanta of excitation, producing a probe wavelength-dependent decay time. Since lower energy probe photons predominantly interrogate higher lying vibrational states, we observe a faster decay of the transient signal at longer wavelengths than at shorter ones.[43]

Figure 4 compares the transient absorption signal of CH_2I_2 in CCl_4 at several probe wavelengths, each fit to the sum of an exponential rise and decay, following excitation of the first and second excited states of the C–H stretch vibration. Figure 5 shows the exponential *decay* times, along with those from measurements at the other excitation levels, and demonstrates that there is a weaker wavelength dependence of the decay times following excitation of the fundamental stretch vibration, ν_s, than for higher levels. Using the description given above, we interpret this difference as a

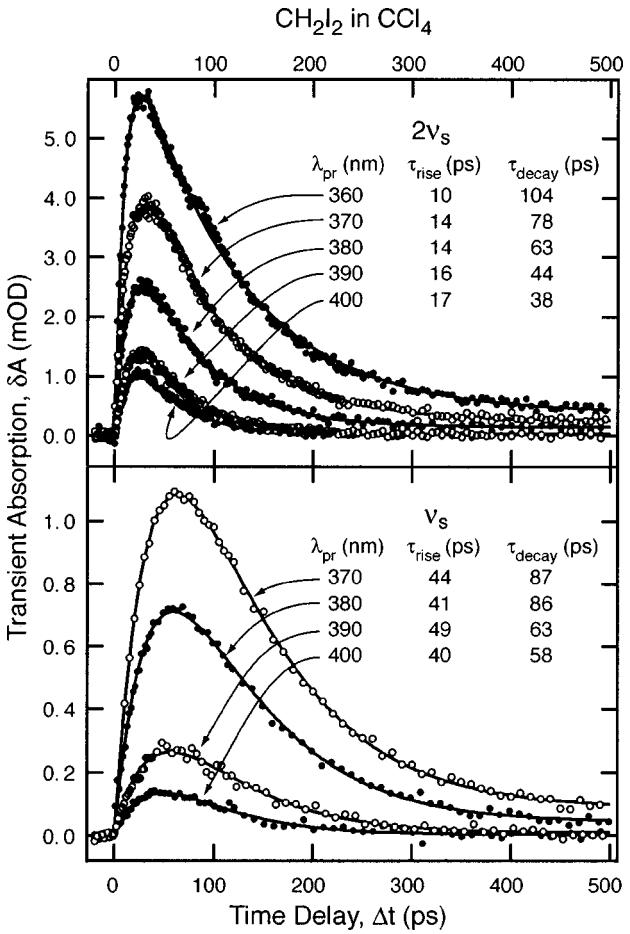

FIG. 4. Transient electronic absorption of CH_2I_2 in CCl_4 at various probe wavelengths following excitation to the C–H stretch fundamental (ν_s) and overtone ($2\nu_s$) levels. The trace at each probe wavelength is fit to the sum of two exponentials.

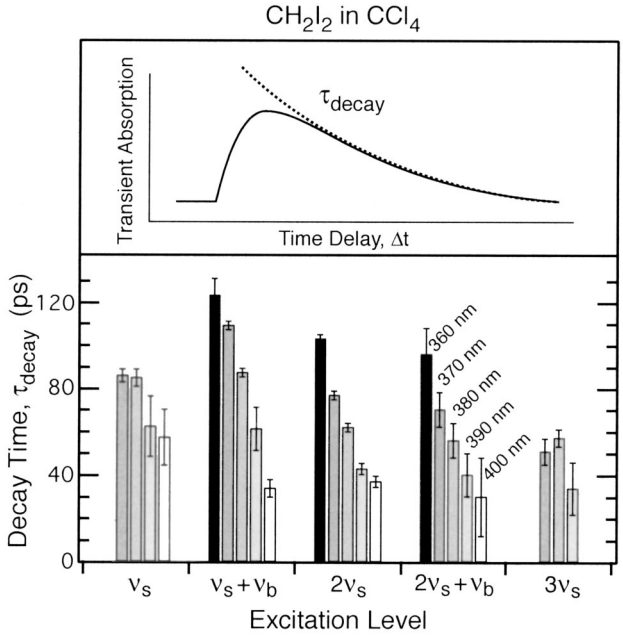

FIG. 5. Exponential decay times of the transient absorption at several probe wavelengths for CH_2I_2 in CCl_4 as a function of the initial excitation level.

change from a predominantly state-specific vibrational energy transfer mechanism at the energy of the C–H stretch fundamental, to a more statistical mechanism at the level of the C–H stretch–bend combination. The slight wavelength dependence at the fundamental vibrational level reflects a minor statistical component underlying the predominantly state-specific IVR mechanism.[44] This minor component is only detectable in the long wavelength transients since they preferentially probe states highly excited in the Franck–Condon active coordinate that are not populated by the primary, state-specific channel. A recent study[45] of vibrational relaxation in the series of iodomethanes (CH_3I, CH_2I_2, and CHI_3) provides additional evidence for state-specific IVR at the fundamental, finding that the vibrational state structure plays a more important role in the relaxation than the density of states.

The decay times following excitation of the $\nu_s+\nu_b$, $2\nu_s$, and $2\nu_s+\nu_b$ bands depend strongly on the probe wavelength, suggesting that the intramolecular relaxation is closer to the statistical limit at each of these initial energy levels. Because the weak infrared absorption at the second overtone, $3\nu_s$, gives a relatively poor signal to noise ratio, it is not possible to infer the vibrational energy transfer mechanism from the wavelength dependence of the decay times. However, we do not expect the mechanism to be different than what we observe at nearby levels of excitation. Our primary conclusion is that the IVR mechanism changes from predominantly state-specific to more nearly statistical for an initial excitation energy between that of the C–H stretch fundamental at 3000 cm^{-1} and the stretch–bend combination at 4400 cm^{-1}.

B. Vibrational energy transfer times

The transient absorption signals directly reflect the population dynamics of the Franck–Condon active vibrational modes in the case of state-specific vibrational energy transfer, as shown in Fig. 3. Thus, for the C–H stretch fundamental we identify the rise time of the signal with intramolecular vibrational relaxation and the decay time with intermolecular energy transfer to the solvent.[48] We obtain the rise and decay times through nonlinear least-square fits of the data at each probe wavelength to a sequential first-order kinetics scheme and average the results to obtain the IVR and IET times. Because data taken at probe wavelengths of 390 nm and longer reflect a minor statistical component of the intramolecular relaxation at the fundamental level, we determine energy transfer times from traces at shorter wavelengths.

The signals recorded at higher initial excitation levels depend strongly on the probe wavelength, as we expect following statistical IVR. We describe the energy transfer for these levels using a population distribution function characterized by a phenomenological time-dependent vibrational temperature, $T_{vib}(t)$.[43] In this model, the observed transient signal, $\delta A(\lambda,t)$, is the difference between room temperature absorption, $A(\lambda,T_0)$, and the absorption at the time-dependent vibrational temperature, $A(\lambda,T_{vib}(t))$. We model the long wavelength portion of the electronic absorption spectrum of CH_2I_2 with an empirical formula[49] that de-

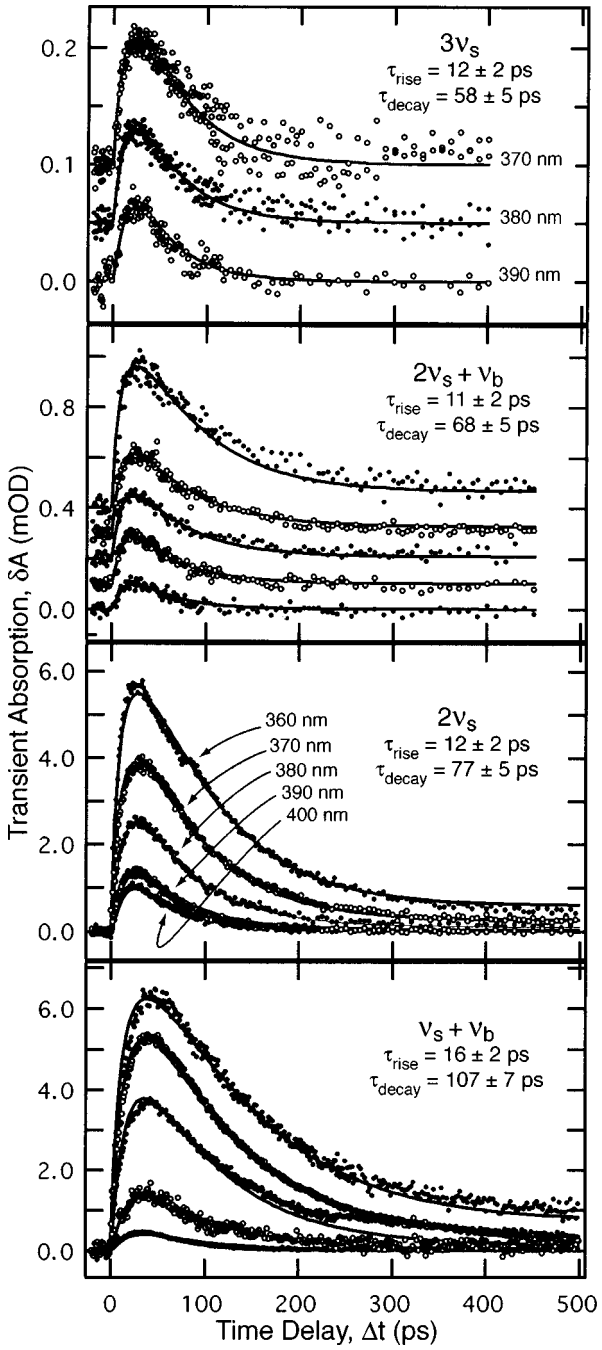

FIG. 6. Transient electronic absorption of CH_2I_2 in CCl_4 at various probe wavelengths following excitation to the C–H combination bands ($\nu_s+\nu_b$,$2\nu_s+\nu_b$) and stretch overtones ($2\nu_s$,$3\nu_s$). The fit to the data at each excitation level uses the temperature-dependent absorption model described in the text.

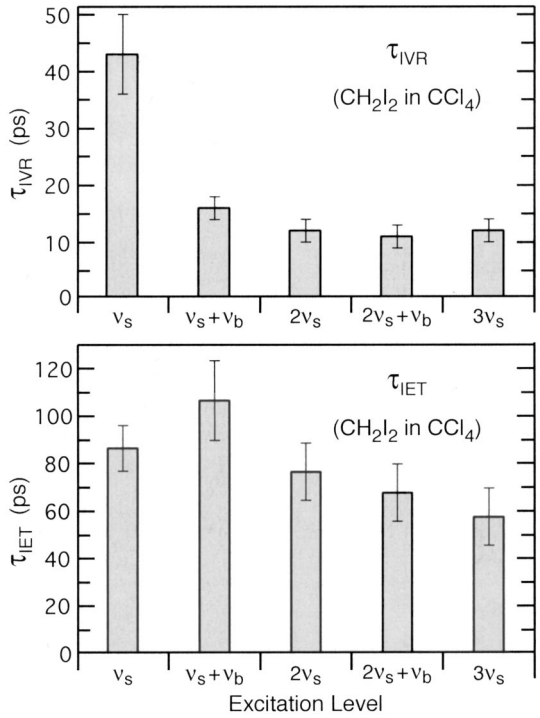

FIG. 7. IVR and IET times for CH_2I_2 in CCl_4 as a function of the initial excitation level.

scribes both the exponential decrease at low frequencies[50] and the Gaussian shape near the absorption maximum,[51] taking into account only the lowest energy electronic transition. Although as many as five electronic transitions appear in the ultraviolet absorption spectrum,[52] the lowest energy band dominates at long wavelengths. The temperature-dependent parameters for the absorption are extrapolations from spectra taken over the temperature range of 284–322 K. Recent 400 nm absorption measurements of CH_2I_2 heated in shock-waves show that the extrapolation may underestimate the change,[46] but since the vibrational temperature is a phenomenological parameter describing the vibrational energy content in the Franck–Condon active modes, the model adequately characterizes the change in absorption during energy transfer.

We model the time evolution of the vibrational temperature with an exponential rise and decay, representing IVR and IET, and use the temperature-dependent absorption spectrum to obtain the resulting signal at each probe wavelength. Fitting the data simultaneously for *all* probe wavelengths at a given excitation level yields the IVR and IET times, as well as a maximum vibrational temperature. (An amplitude scaling factor compensates for small changes in the experimental conditions among the traces.) The maximum vibrational temperature is typically close to 1000 K, which is consistent with the amount of energy initially deposited.[43] Additionally, an exponentially rising temperature offset compensates for solvent heating by the pump laser pulse, with this solvent rise time set equal to the vibrational population decay time of the solute. Figure 6 shows the result of nonlinear least square fits to the experimental data, at vibrational levels above the C–H stretch fundamental, for CH_2I_2 in CCl_4 using the temperature model. The model reproduces the experimental data very well for the $2\nu_s$, $2\nu_s+\nu_b$, and $3\nu_s$ excitation levels. The fit to the transient absorption traces after excitation to the $\nu_s+\nu_b$ stretch–bend combination band is not as good, perhaps reflecting a component of state-specific IVR. This behavior, along with the observation of a minor statistical component at the fundamental, is consistent with a gradual transition from state-specific to more nearly statistical relaxation. A gradual transition between the two mechanisms is not surprising since they are limiting cases. Figure 7 summa-

TABLE I. Intramolecular vibrational relaxation (IVR) times for CH_2I_2 in various solvents.

Excitation	Energy (cm^{-1})	CCl_4 (ps)	$CDCl_3$ (ps)	C_6D_6 (ps)	$(CD_3)_2CO$ (ps)
ν_s	~3000	43±7	33±3	15±1	14±4
$\nu_s+\nu_b$	~4400	16±2	14±2	6±1[a]	5±1
$2\nu_s$	~6000	12±2	11±1	9±1	5±1

[a]In C_6H_6.

rizes the vibrational energy transfer times obtained from the fits at all excitation levels for CH_2I_2 in CCl_4, and Tables I and II give the IVR and IET times for CH_2I_2 in various solvents.

1. Intramolecular vibrational relaxation

The Golden Rule expression [Eq. (1)] predicts that the intramolecular vibrational relaxation rate in the statistical regime scales linearly with the state density, which itself increases rapidly with vibrational energy. However, Fig. 8 shows that the IVR rate does not increase for excitation energies above the first C–H stretch overtone ($2\nu_s$), around 6000 cm^{-1}, even though the total density of states increases from 16 states/cm^{-1} at $2\nu_s$ to 124 states/cm^{-1} at $3\nu_s$. (The total density of states, middle panel of Fig. 8, is from a direct harmonic state count using the frequencies listed in Table III.[53]) Insensitivity of the IVR rate to the total density of states suggests that the additional states available at higher excitation levels do not contribute to the initial vibrational relaxation. The extra states apparently constitute higher tiers of weakly coupled states, while the first tier of accepting states is similar at each excitation level and consists of those states that are most important for the initial relaxation. Since the coupling strength between two states generally decreases as the number of quanta exchanged in the transition increases, we analyze the intramolecular relaxation in terms of the coupling order, *n*, connecting the states. This is similar to previous work that associates IVR with the coupling order between states.[23–25,45,54–58] States with a high coupling order, which are weakly coupled to the initially excited state, compose higher tiers in the IVR hierarchy, while states with low coupling order make up the lower tiers. We enumerate the states that are coupled to the initially excited C–H stretch or stretch–bend states at a particular order, and define the order-specific density of states, $\rho_n(E)$, as the density of those states coupled to the initially excited state at order *n*. Classifying all states with the same coupling order into one category makes the overly simple assumption that the coupling strength, *V*, is the same for all states with a specific coupling order.

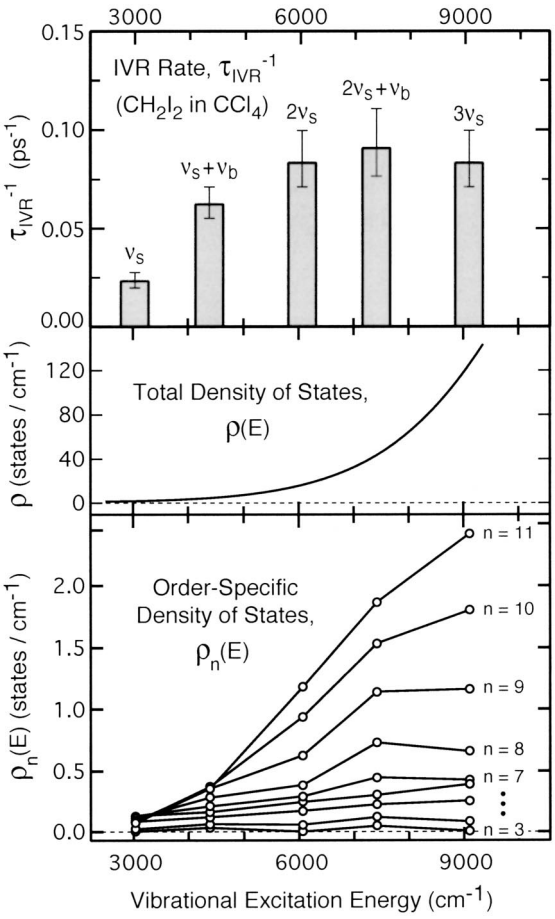

FIG. 8. Top: intramolecular vibrational relaxation rate, τ_{IVR}^{-1}, for CH_2I_2 in CCl_4 at each initial vibrational excitation level. Middle: total density of states, ρ, as a function of vibrational energy, *E*. Bottom: order-specific density of states, $\rho_n(E)$, at each vibrational excitation level for a few orders of coupling, *n*.

The bottom panel of Fig. 8 shows how the order-specific density of states changes with the vibrational energy level for a few orders of coupling. At low order, $\rho_n(E)$ remains relatively constant over the energy range shown, but at higher coupling order it increases rapidly with energy. We associate this difference in behavior with the stagnation of IVR times for CH_2I_2 at energies above the $2\nu_s$ overtone. Figure 8

TABLE II. Intermolecular energy transfer (IET) times for CH_2I_2 in various solvents.

Excitation	Energy (cm^{-1})	CCl_4 (ps)	$CDCl_3$ (ps)	C_6D_6 (ps)	$(CD_3)_2CO$ (ps)
ν_s	~3000	87±4	84±4	42±3	22±5
$\nu_s+\nu_b$	~4400	107±7	102±7	30±3[a]	33±3
$2\nu_s$	~6000	77±5	53±3	24±2	17±2

[a]In C_6H_6.

TABLE III. Normal mode frequencies and symmetries for CH_2I_2.[a]

Mode	Motion	Energy (cm^{-1})	Symmetry
ν_1	CH_2 sym. stretch	2992	a_1
ν_2	CH_2 bend	1350	a_1
ν_3	CI_2 sym. stretch	484	a_1
ν_4	CI_2 bend	127	a_1
ν_5	CH_2 twist	1031	a_2
ν_6	CH_2 antisym. stretch	3069	b_1
ν_7	CH_2 rock	716	b_1
ν_8	CH_2 wag	1105	b_2
ν_9	CI_2 antisym. stretch	570	b_2

[a]Reference 53.

shows that $\rho_n(E)$ is relatively constant above 6000 cm^{-1} for $n \leqslant 7$ but increases with energy for eighth and higher order coupling. Thus, we infer that states coupled to the initially excited state in about seventh order and lower dominate the intramolecular energy flow. This situation is analogous to previous work showing that low order resonances can dominate the IVR even when the relaxation involves a large number of states.[23–25]

2. Intermolecular energy transfer

The mechanism and rate of intermolecular energy transfer depend not only on the surrounding environment but also on the internal modes of the relaxing molecule and their coupling to the solvent. Molecular dynamics simulations by Kab *et al.*[59] find that the dominant gateway mode of CH_2I_2 in $CDCl_3$ is the CH_2 rocking vibration, not the lower frequency C–I stretch and bend modes. Although this conclusion contradicts the notion that the lowest frequency modes are the most strongly coupled to the solvent,[5] it is consistent with recent experimental evidence that low frequency modes are not necessarily the gateway modes.[25] Our experiment is only sensitive to the Franck–Condon active (primarily C–I stretch) modes and cannot determine which modes transfer energy to the solvent most efficiently. Regardless of the transfer mechanism, we observe intermolecular energy transfer by monitoring the decay of vibrational population in the modes to which our probe is sensitive.

We assume that IET produces a single exponential decay of the signal, independent of a state-specific or a statistical IVR mechanism. The lower panel of Fig. 7 shows these decay times for CH_2I_2 in CCl_4 following excitation to the various C–H stretch and stretch–bend levels between 3000 and 9000 cm^{-1}. We observe a slight decrease in the intermolecular energy transfer time for increasing levels of initial excitation, with an unexpectedly short transfer time for the ν_s fundamental. The energy level dependence of the IET time indicates that a single exponential decay does not completely describe the energy transfer, but instead approximates the actual, energy-dependent relaxation. The IET rate depends on the level of excitation in the modes that we probe since vibrational relaxation rates increase with the quantum number.[60] Higher levels of initial C–H excitation lead to more vibrational quanta in the Franck–Condon active modes, and the *average* IET time that we observe reflects the faster initial relaxation. The result is a modest decrease in IET times with increasing level of initial excitation.

Charvat *et al.*[47] treat the excitation level dependence of the intermolecular energy transfer times with a biexponential decay function, and find that time constants of 27 and 140 ps reproduce the vibrational relaxation in CCl_4 following excitation of both the $\nu_s+\nu_b$ combination and the $2\nu_s$ overtone. (They find that the IVR and IET times are the same for both the $\nu_2+\nu_6$ and $\nu_1+\nu_8/\nu_5+\nu_6$ combination bands, which we collectively call $\nu_s+\nu_b$.) The biexponential decay provides a slightly better fit of the data because it begins to account for the energy level dependence of the relaxation rate constant, but it is still only an approximate treatment of the energy transfer to solution. In terms of our picture, the two decay times correspond to the average relaxation rate of Franck–Condon active modes that are either highly excited or contain only a few quanta of excitation.

The intermolecular energy transfer time for the ν_s fundamental is shorter than extrapolation from higher levels of initial excitation suggests. This surprising behavior may arise from an acceleration of the intermolecular energy transfer following state-specific redistribution within the molecule. The state-specific IVR mechanism could directly populate a larger fraction of gateway modes than the more random vibrational distribution produced by statistical IVR. Since the gateway modes transfer energy to the solvent quickly and directly, a distribution containing a large fraction of these modes relaxes more rapidly than one with a small fraction of excited gateway modes, producing an IET rate at the fundamental level that is faster than at higher levels. Our observation that the ν_s fundamental level has a shorter intermolecular relaxation time than the $\nu_s+\nu_b$ combination in other solvents as well (see Table II) supports this interpretation.

C. Solvent dependence

The solvent plays an essential role in the vibrational energy transfer that we observe. Tables I and II list the IVR and IET times, respectively, for CH_2I_2 in the solvents CCl_4, $CDCl_3$, C_6D_6, C_6H_6, and $(CD_3)_2CO$ following excitation of the ν_s fundamental, the $\nu_s+\nu_b$ combination, and the $2\nu_s$ overtone levels. We choose deuterated solvents to avoid direct excitation of solvent modes by the infrared pump pulse at the C–H absorption frequencies. (Because the $\nu_s+\nu_b$ combination band for CH_2I_2 coincides with an absorption in C_6D_6 but not C_6H_6, we use nondeuterated benzene for experiments on that state.) For each of the vibrational excitation levels, the strongly interacting solvents accelerate both intramolecular vibrational relaxation and intermolecular energy transfer, consistent with previous qualitative interpretations.[43,44,46] Specifically, the presence of a dipole moment in $CDCl_3$ does not significantly change the IVR or IET times compared to the nonpolar solvent CCl_4, but nearest neighbor interactions of solvent molecules with CH_2I_2, such as the $\pi \rightarrow \sigma^*_{C-I}$ charge transfer in the case of benzene and $n_O \rightarrow \sigma^*_{C-I}$ for acetone, have a large effect on the energy transfer times. Relaxation times following excitation of the $2\nu_s$ overtone of CH_2I_2 in supercritical CO_2 by Sekiguchi *et al.*[61] provide another reference point. They find that changing the solvent density has no apparent effect on intramolecular vibrational relaxation but strongly influences the intermolecular energy transfer.

The effect of different solvents on the intramolecular vibrational relaxation times is particularly interesting because it provides direct evidence of solvent-assisted IVR. Table I clearly shows that the more strongly interacting solvents accelerate the intramolecular relaxation at all excitation levels but does not indicate the IVR times in the absence of solvent. The $2\nu_s$ overtone relaxation measurements[61] in supercritical CO_2 give a relaxation time of 15 ps that is comparable to our measurement of 12 ps in CCl_4, the most weakly interacting solvent studied. This similarity suggests that the intramolecular energy transfer time of isolated CH_2I_2 may not be very

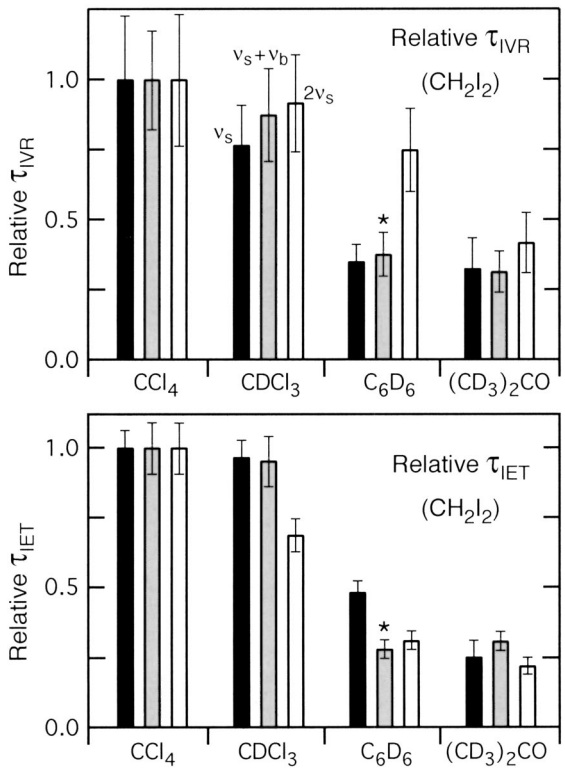

FIG. 9. Relative IVR and IET times (scaled to the value in CCl_4) for the ν_s, $\nu_s+\nu_b$, and $2\nu_s$ excitation levels as a function of the solvent. The asterisk denotes that C_6H_6 is the solvent.

different, but measurements in the gas phase are necessary to completely separate the solvent environment from the IVR process.

Our data show that the initial excitation level has little or no effect on the solvent dependence of intramolecular vibrational relaxation and intermolecular energy transfer. Since the absolute energy transfer times depend strongly on the initial excitation level, trends are not immediately obvious from the values in Tables I and II. Thus, in Fig. 9 we scale the energy transfer times of all solvents relative to that of CCl_4 for each excitation level. The similar variation with solvent at all levels of excitation indicates that solvent interactions enhance IVR and IET of CH_2I_2 in solution independent of the initial excitation level. The more strongly interacting solvents produce consistently faster intramolecular vibrational relaxation and intermolecular energy transfer.

IV. CONCLUSION

Transient electronic absorption measures IVR and IET for CH_2I_2 in solution following excitation of C–H stretch and stretch–bend modes at energies between 3000 and 9000 cm^{-1}. Specifically, we observe the effect of the excitation level on the IVR mechanism, the IVR and IET times, and the solvent dependence. The probe wavelength dependence of the transient absorption signals shows that intramolecular vibrational relaxation is predominantly state-specific at the fundamental excitation level but is closer to the statistical limit at higher energies. In the case of the statistical mechanism, we extract IVR and IET times with a model based on the experimentally determined temperature dependence of the electronic absorption spectrum. The intramolecular vibrational relaxation times depend strongly on the excitation energy for states between the fundamental level and the first overtone but are constant at energies above the overtone, indicating that the additional vibrational states available at higher energy levels do not participate in the intramolecular relaxation. We use an order-specific density of states, $\rho_n(E)$, to interpret these results and infer that IVR in CH_2I_2 occurs predominantly through states that are fewer than about eight orders of coupling away from the initially excited state. The intermolecular energy transfer times depend weakly on the excitation energy, probably because of the different levels of excitation in the Franck–Condon active modes populated by intramolecular relaxation. Although the solvent has a strong influence on the absolute IVR and IET times, there is no evidence that this effect depends on the initial excitation level.

ACKNOWLEDGMENT

The authors thank the Air Force Office of Scientific Research for support of this work.

[1] T. Baer and W. L. Hase, *Unimolecular Reaction Dynamics* (Oxford University Press, New York, 1996).
[2] F. F. Crim, J. Phys. Chem. **100**, 12725 (1996).
[3] A. Seilmeier and W. Kaiser, in *Ultrashort Laser Pulses*, edited by W. Kaiser (Springer-Verlag, Berlin, 1988), Vol. 60, p. 279.
[4] T. Elsaesser and W. Kaiser, Annu. Rev. Phys. Chem. **42**, 83 (1991).
[5] J. C. Owrutsky, D. Raftery, and R. M. Hochstrasser, Annu. Rev. Phys. Chem. **45**, 519 (1994).
[6] D. W. Oxtoby, Adv. Chem. Phys. **47**, 487 (1981).
[7] V. M. Kenkre, A. Tokmakoff, and M. D. Fayer, J. Chem. Phys. **101**, 10618 (1994).
[8] S. A. Egorov and J. L. Skinner, J. Chem. Phys. **112**, 275 (2000).
[9] P. R. Stannard and W. M. Gelbart, J. Phys. Chem. **85**, 3592 (1981).
[10] K. K. Lehmann, G. Scoles, and B. H. Pate, Annu. Rev. Phys. Chem. **45**, 241 (1994).
[11] D. J. Nesbitt and R. W. Field, J. Phys. Chem. **100**, 12735 (1996).
[12] K. F. Freed and A. Nitzan, J. Chem. Phys. **73**, 4765 (1980).
[13] P. M. Felker and A. H. Zewail, J. Chem. Phys. **82**, 2975 (1985).
[14] P. M. Felker, W. R. Lambert, and A. H. Zewail, J. Chem. Phys. **82**, 3003 (1985).
[15] J. S. Baskin, P. M. Felker, and A. H. Zewail, J. Chem. Phys. **86**, 2483 (1987).
[16] J. F. Kauffman, M. J. Cote, P. G. Smith, and J. D. Mcdonald, J. Chem. Phys. **90**, 2874 (1989).
[17] P. G. Smith and J. D. McDonald, J. Chem. Phys. **92**, 1004 (1990).
[18] X. Zhang, J. M. Smith, and J. L. Knee, J. Chem. Phys. **100**, 2429 (1994).
[19] C. Cohen-Tannoudji, B. Diu, and F. Laloë, *Quantum Mechanics* (Wiley, New York, 1977).
[20] R. G. Bray and M. J. Berry, J. Chem. Phys. **71**, 4909 (1979).
[21] K. V. Reddy, D. F. Heller, and M. J. Berry, J. Chem. Phys. **76**, 2814 (1982).
[22] E. R. T. Kerstel, K. K. Lehmann, T. F. Mentel, B. H. Pate, and G. Scoles, J. Phys. Chem. **95**, 8282 (1991).
[23] J. E. Gambogi, R. P. L'Esperance, K. K. Lehmann, B. H. Pate, and G. Scoles, J. Chem. Phys. **98**, 1116 (1993).
[24] J. E. Gambogi, K. K. Lehmann, B. H. Pate, G. Scoles, and X. M. Yang, J. Chem. Phys. **98**, 1748 (1993).
[25] J. Assmann, A. Charvat, D. Schwarzer, C. Kappel, K. Luther, and B. Abel, J. Phys. Chem. A **106**, 5197 (2002).
[26] G. A. Voth, J. Chem. Phys. **88**, 5547 (1988).
[27] A. Laubereau, D. V. D. Linde, and W. Kaiser, Phys. Rev. Lett. **28**, 1162 (1972).
[28] K. Spanner, A. Laubereau, and W. Kaiser, Chem. Phys. Lett. **44**, 88 (1976).

[29] A. Laubereau, S. F. Fischer, K. Spanner, and W. Kaiser, Chem. Phys. **31**, 335 (1978).
[30] H. Graener and A. Laubereau, Appl. Phys. B: Photophys. Laser Chem. **B29**, 213 (1982).
[31] F. Wondrazek, A. Seilmeier, and W. Kaiser, Chem. Phys. Lett. **104**, 121 (1984).
[32] W. Kaiser, Ber. Bunsenges. Phys. Chem. **89**, 213 (1985).
[33] H. J. Bakker, P. C. M. Planken, and A. Lagendijk, Nature (London) **347**, 745 (1990).
[34] H. J. Bakker, P. C. M. Planken, and A. Lagendijk, J. Chem. Phys. **94**, 6007 (1991).
[35] H. J. Bakker, J. Chem. Phys. **98**, 8496 (1993).
[36] X. Y. Hong, S. Chen, and D. D. Dlott, J. Phys. Chem. **99**, 9102 (1995).
[37] J. C. Deak, L. K. Iwaki, and D. D. Dlott, J. Phys. Chem. A **102**, 8193 (1998).
[38] L. K. Iwaki and D. D. Dlott, J. Phys. Chem. A **104**, 9101 (2000).
[39] H. Graener, R. Zurl, and M. Hofmann, J. Phys. Chem. B **101**, 1745 (1997).
[40] G. Seifert, R. Zurl, and H. Graener, J. Phys. Chem. A **103**, 10749 (1999).
[41] R. M. Stratt and M. Maroncelli, J. Phys. Chem. **100**, 12981 (1996).
[42] D. Vanden Bout, J. E. Freitas, and M. Berg, Chem. Phys. Lett. **229**, 87 (1994).
[43] D. Bingemann, A. M. King, and F. F. Crim, J. Chem. Phys. **113**, 5018 (2000).
[44] C. M. Cheatum, M. M. Heckscher, D. Bingemann, and F. F. Crim, J. Chem. Phys. **115**, 7086 (2001).
[45] M. M. Heckscher, L. Sheps, D. Bingemann, and F. F. Crim, J. Chem. Phys. **117**, 8917 (2002).
[46] A. Charvat, J. Assmann, B. Abel, and D. Schwarzer, J. Phys. Chem. A **105**, 5071 (2001).
[47] A. Charvat, J. Assmann, B. Abel, D. Schwarzer, K. Henning, K. Luther, and J. Troe, Phys. Chem. Chem. Phys. **3**, 2230 (2001).
[48] The rise of the transient absorption signal corresponds to the faster process, and the decay corresponds to the slower process, regardless of which is IVR or IET. We assign the rise as IVR and the decay as IET based on previous results at the fundamental (Refs. 34 and 45) and the probe wavelength dependence of the decay at higher excitation levels.
[49] H. Mahr, Phys. Rev. **132**, 1880 (1963).
[50] F. Urbach, Phys. Rev. **92**, 1324 (1953).
[51] J. A. Joens, J. Phys. Chem. **98**, 1394 (1994).
[52] J. Zhang and D. G. Imre, J. Chem. Phys. **89**, 309 (1988).
[53] M. P. Marzocchi, V. Schettino, and S. Califano, J. Chem. Phys. **45**, 1400 (1966).
[54] R. Pearman and M. Gruebele, J. Chem. Phys. **108**, 6561 (1998).
[55] M. Gruebele and R. Bigwood, Int. Rev. Phys. Chem. **17**, 91 (1998).
[56] M. Gruebele, Adv. Chem. Phys. **114**, 193 (2001).
[57] E. J. Heilweil, R. R. Cavanagh, and J. C. Stephenson, Chem. Phys. Lett. **134**, 181 (1987).
[58] E. J. Heilweil, M. P. Casassa, R. R. Cavanagh, and J. C. Stephenson, J. Chem. Phys. **85**, 5004 (1986).
[59] G. Kab, C. Schroder, and D. Schwarzer, Phys. Chem. Chem. Phys. **4**, 271 (2002).
[60] J. T. Yardley, *Introduction to Molecular Energy Transfer* (Academic, New York, 1980).
[61] K. Sekiguchi, A. Shimojima, and O. Kajimoto, Chem. Phys. Lett. **356**, 84 (2002).